Supporting Information

Evolution from single relaxation process to two-step relaxation processes of Dy_2 single-molecule magnets via the modulations of the terminal solvent ligands

Dawei Li,[a] Man-Man Ding,[b] Yuan Huang,[a] David Felipe Tello Yepes,[d] Haiyan Li,[a] Yahong Li,*[a] Yi-Quan Zhang,*[b] and Jinlei Yao*[c]

[a]*College of Chemistry, Chemical Engineering and Materials Science, Soochow University, Suzhou 215123, P. R. China. E-mail: liyahong@suda.edu.cn*

[b]*Jiangsu Key Laboratory for NSLSCS, School of Physical Science and Technology, Nanjing Normal University, Nanjing 210023, P. R. China. E-mail: zhangyiquan@njnu.edu.cn*

[c]*Jiangsu Key Laboratory of Micro and Nano Heat Fluid Flow Technology and Energy Application, School of Physical Science and Technology, Suzhou University of Science and Technology, Suzhou 215009, P. R. China. E-mail: jlyao@usts.edu.cn*

[d]*College of Environmental Engineering, University of Waterloo, Waterloo N2L3G1, Canada*

Supplementary Information Contents

1. ^{1}H, ^{13}C NMR spectra of H_2L

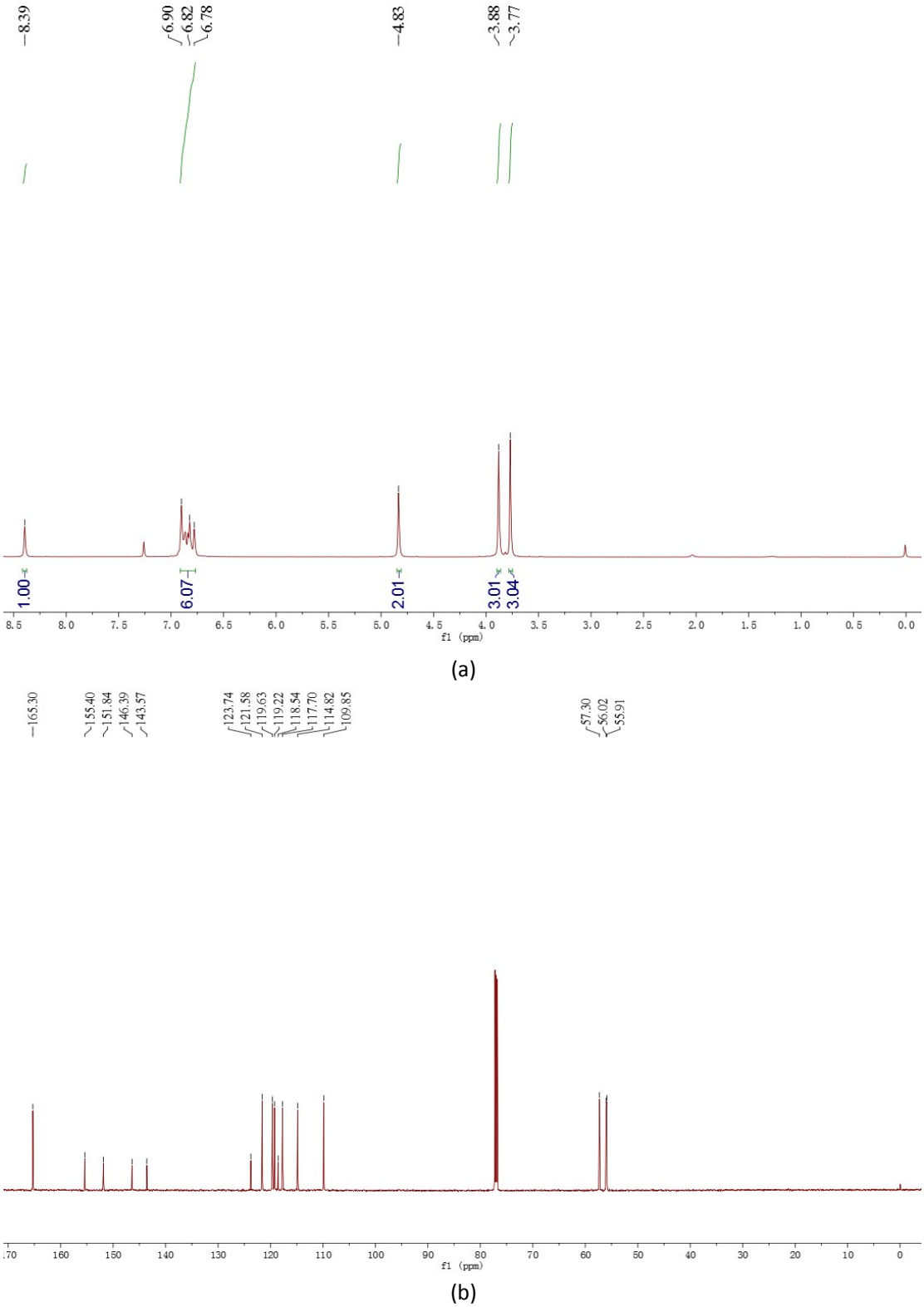

Fig. S1. The ^{1}H NMR (a) and ^{13}C NMR (b) spectra of H_2L.

2. PXRD patterns of 1-3

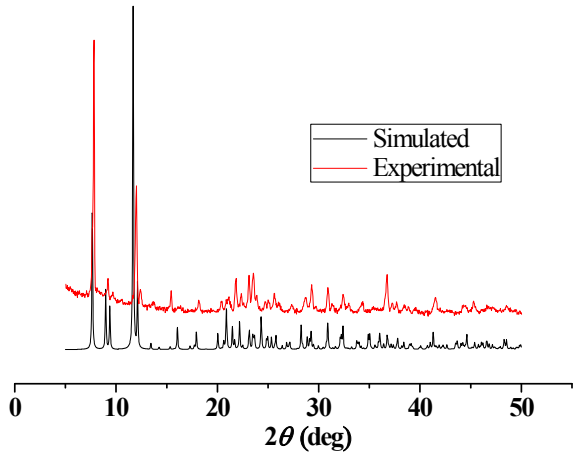

(a)

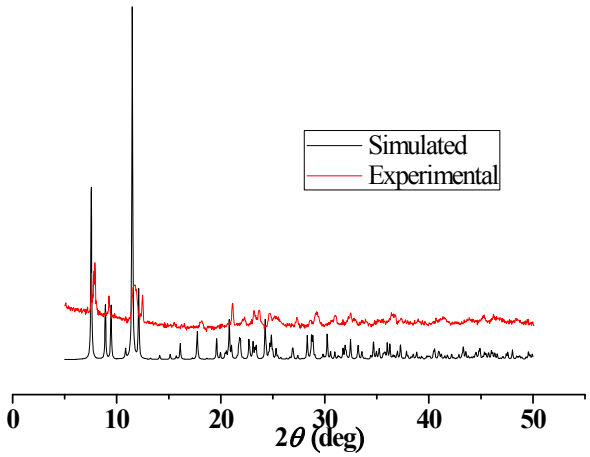

(b)

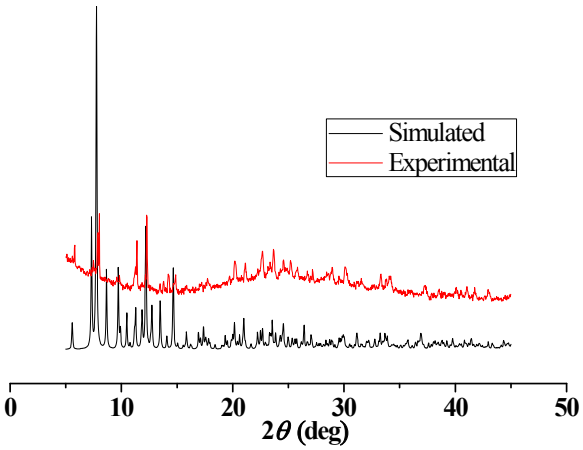

(c)

Fig. S2. PXRD patterns of **1** (a), **2** (b) and **3** (c).

3. IR spectra of H_2L and 1-3

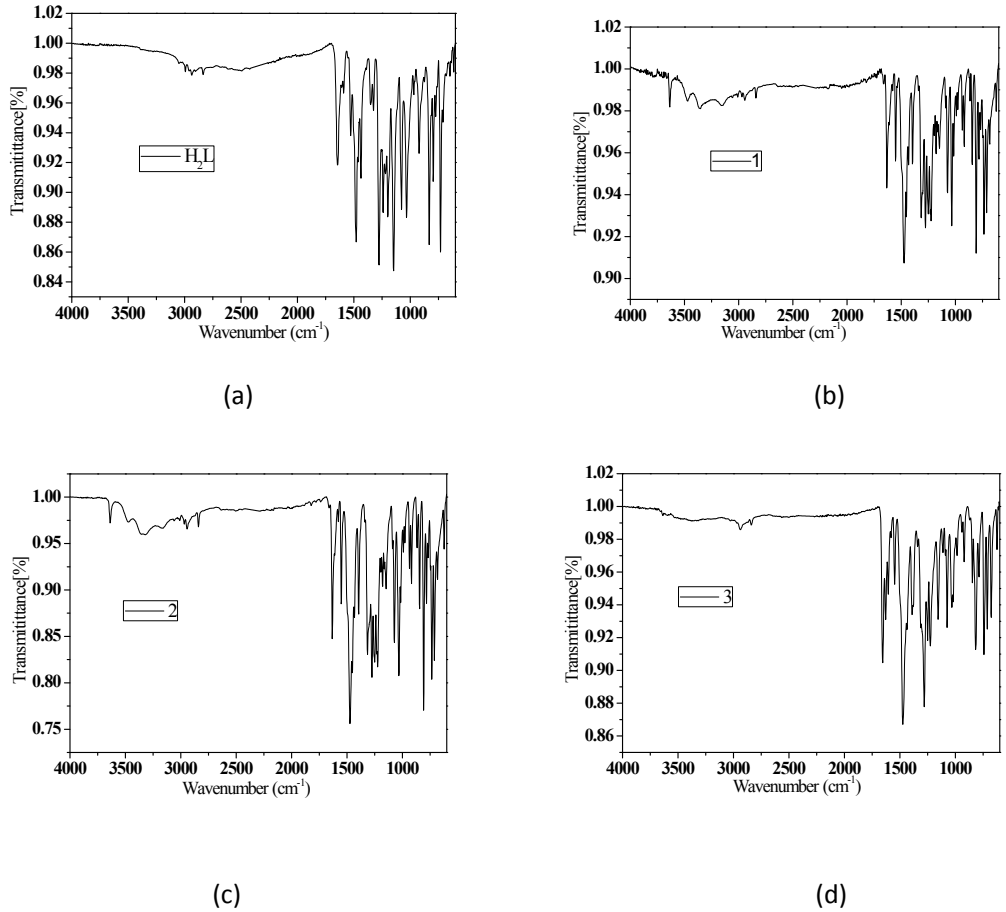

Fig. S3. FT-IR spectra of H_2L, **1** (a), **2** (b) and **3** (c).

4. Crystal date and structure refinement detail for 1-3

Table S1. Crystal and structure refinement data for **1-3**

	1	**2**	**3**
Empirical formula	$C_{34}H_{38}Dy_2N_4O_{16}$	$C_{36}H_{42}Dy_2N_4O_{16}$	$C_{39}H_{47}Dy_2N_6O_{16.5}$
Temperature/K	296.15	296.15	296.15
Formula weigh	1083.68	1111.73	1188.84
Crystal system	orthorhombic	orthorhombic	monoclinic
Space group	*Pbcn*	*Pbcn*	$P2_1/c$
a/Å	18.8341(9)	18.6721(16)	16.0720(14)
b/Å	8.8537(4)	9.0807(8)	16.4037(14)
c/Å	23.0950(12)	23.3406(19)	18.1256(16)
α/°	90	90	90
β/°	90	90	100.123(2)
γ/°	90	90	90
Volume/Å^3	3851.1(3)	3957.5(6)	4704.2(7)
Z	4	4	4
ρ_{calc}/g cm^{-3}	1.869	1.866	1.646
μ/mm^{-1}	3.927	3.824	3.223
F(000)	2120.0	2184.0	2296.0
Crystal size/mm^3	0.2 × 0.08 × 0.06	0.12 × 0.08 × 0.08	0.3 × 0.05 × 0.03
θ range/°	5.084 to 50	4.988 to 55.252	5.15 to 55.168
Index ranges	$-18 \le h \le 22$	$-24 \le h \le 24$	$-20 \le h \le 18$
	$-8 \le k \le 10$	$-11 \le k \le 7$	$-20 \le k \le 18$
	$-13 \le l \le 27$	$-28 \le l \le 30$	$-19 \le l \le 23$
Reflections collected	10639	13824	28271
Independent reflections	3397 [*R*(int) = 0.0813]	4557 [*R*(int) = 0.0466]	10601 [*R*(int) = 0.0532]
Data/restraints/parameters	3397/4/259	4557/3/268	10601/36/584
Goodness-of-fit on F^2	1.010	1.078	1.058
Final *R* indexes	R_1 = 0.0484	R_1 = 0.0445	R_1 = 0.0590
[I ≥ 2σ(I)]	wR_2 = 0.1000	wR_2 = 0.1181	wR_2 = 0.1515
Final *R* indexes	R_1 = 0.0981	R_1 = 0.0701	R_1 = 0.1154
[all data]	wR_2 = 0.1106	wR_2 = 0.1323	wR_2 = 0.1848
Largest diff. peak/hole/ eÅ^{-3}	1.40/-0.78	2.05/-1.40	2.84/-1.37

5. Selected bond lengths and angles for 1-3

Table S2. Selected bond lengths (Å) and angle (°) for complexes **1-3**

1			
Dy1-N1	2.428(7)	Dy1-O3[1]	2.504(5)
Dy1-O2	2.309(6)	Dy1-O1	2.161(6)
Dy1-O2[1]	2.347(5)	Dy1-O5	2.371(7)
Dy1-O6	2.422(7)	O2-Dy1[1]	2.347(5)
Dy1-O7	2.486(6)	O3-Dy1[1]	2.504(5)
N1-Dy1-O7	75.0(2)	O6-Dy1-O7	52.3(2)
N1-Dy1-O3[1]	147.6(2)	O6-Dy1-O3[1]	69.9(2)
O2[1]-Dy1-N1	134.1(2)	O7-Dy1-O3[1]	120.5(2)
O2-Dy1-N1	78.1(2)	O1-Dy1-N1	74.8(2)
O2-Dy1-O2[1]	67.3(2)	O1-Dy1-O2[1]	143.23(19)
O2[1]-Dy1-O6	90.0(2)	O1-Dy1-O2	149.40(19)
O2-Dy1-O6	99.0(2)	O1-Dy1-O6	85.7(2)
O2-Dy1-O7	75.7(2)	O1-Dy1-O7	83.9(2)
O2[1]-Dy1-O7	121.3(2)	O1-Dy1-O3[1]	78.85(19)
O2[1]-Dy1-O3[1]	65.48(18)	O1-Dy1-O5	86.2(2)
O2-Dy1-O3[1]	131.25(18)	O5-Dy1-N1	80.1(2)
O2-Dy1-O5	102.8(2)	O5-Dy1-O6	149.5(2)
O2[1]-Dy1-O5	79.3(2)	O5-Dy1-O7	154.9(2)
O6-Dy1-N1	125.5(2)	O5-Dy1-O3[1]	79.8(2)
Dy1-O2-Dy1[1]	106.4(2)		

[1]-X,+Y,1/2-Z

2			
Dy1-O2	2.329(4)	Dy1-O5	2.391(5)
Dy1-O2[1]	2.312(5)	Dy1-O6	2.414(6)
Dy1-O3	2.510(5)	O2-Dy1[1]	2.312(5)
Dy1-O1[1]	2.159(5)	O1-Dy1[1]	2.159(5)
Dy1-O7	2.462(5)	N1-Dy1[1]	2.439(5)
Dy1-N1[1]	2.440(5)	O1[1]-Dy1-O7	84.2(2)
O2[1]-Dy1-O2	67.08(18)	O1[1]-Dy1-N1[1]	75.66(18)
O2[1]-Dy1-O3	130.83(16)	O1[1]-Dy1-O5	86.0(2)
O2-Dy1-O3	65.64(16)	O1[1]-Dy1-O6	86.7(2)
O2-Dy1-O7	122.18(18)	O7-Dy1-O3	120.97(18)
O2[1]-Dy1-O7	75.21(18)	N1[1]-Dy1-O3	148.84(18)
O2[1]-Dy1-N1[1]	77.45(17)	N1[1]-Dy1-O7	74.04(19)
O2-Dy1-N1[1]	132.83(18)	O5-Dy1-O3	79.82(19)
O2-Dy1-O5	78.28(17)	O5-Dy1-O7	154.52(18)
O2[1]-Dy1-O5	103.18(19)	O5-Dy1-N1[1]	80.76(19)

O2[1]-Dy1-O6	97.4(2)	O5-Dy1-O6	150.5(2)
O2-Dy1-O6	90.8(2)	O6-Dy1-O3	70.76(19)
O1[1]-Dy1-O2	143.08(18)	O6-Dy1-O7	52.02(19)
O1[1]-Dy1-O2[1]	149.73(17)	O6-Dy1-N1[1]	124.7(2)
O1[1]-Dy1-O3	78.88(17)	Dy1[1]-O2-Dy1	106.84(17)

[1]1-X,+Y,1/2-Z

3			
Dy1A-Dy1	3.7987(5)	Dy1-O2A	2.297(4)
Dy1A-O2A	2.341(5)	Dy1-O2	2.323(5)
Dy1A-O2	2.354(4)	Dy1-O1	2.182(5)
Dy1A-O1A	2.167(5)	Dy1-O5	2.285(6)
Dy1A-O3	2.476(5)	Dy1-O3A	2.473(6)
Dy1A-O5A	2.313(6)	Dy1-N1	2.480(6)
Dy1A-O6A	2.444(6)	Dy1-O7	2.427(6)
Dy1A-N1A	2.472(6)	Dy1-O6	2.460(7)
Dy1A-O7A	2.488(6)	Dy1-N3	2.869(10)
Dy1A-N3A	2.871(8)	O2A-Dy1-Dy1A	35.39(11)
O2A-Dy1A-Dy1	34.64(10)	O2A-Dy1-O2	71.16(16)
O2A-Dy1A-O2	69.88(15)	O2A-Dy1-O3A	65.41(18)
O2A-Dy1A-O3	124.58(16)	O2A-Dy1-N1	146.47(19)
O2A-Dy1A-O6A	79.8(2)	O2A-Dy1-O7	89.33(19)
O2A-Dy1A-N1A	78.52(18)	O2A-Dy1-O6	75.4(2)
O2A-Dy1A-O7A	122.6(2)	O2A-Dy1-N3	81.0(2)
O2A-Dy1A-N3A	101.3(3)	O2-Dy1-Dy1A	35.96(11)
O2-Dy1A-Dy1	35.43(12)	O2-Dy1-O3A	125.15(19)
O2-Dy1A-O3	65.28(16)	O2-Dy1-N1	76.95(18)
O2-Dy1A-O6A	85.49(19)	O2-Dy1-O7	81.9(2)
O2-Dy1A-N1A	145.64(19)	O2-Dy1-O6	123.4(3)
O2-Dy1A-O7A	77.0(2)	O2-Dy1-N3	102.3(3)
O2-Dy1A-N3A	79.5(2)	O1-Dy1-Dy1A	171.04(17)
O1A-Dy1A-Dy1	169.36(16)	O1-Dy1-O2A	139.47(19)
O1A-Dy1A-O2A	149.08(18)	O1-Dy1-O2	148.84(19)
O1A-Dy1A-O2	139.82(18)	O1-Dy1-O5	84.9(2)
O1A-Dy1A-O3	77.21(18)	O1-Dy1-O3A	77.9(2)
O1A-Dy1A-O5A	85.0(2)	O1-Dy1-N1	73.6(2)
O1A-Dy1A-O6A	106.3(2)	O1-Dy1-O7	100.5(2)
O1A-Dy1A-N1A	73.9(2)	O1-Dy1-O6	79.5(3)
O1A-Dy1A-O7A	81.0(2)	O1-Dy1-N3	90.9(3)
O1A-Dy1A-N3A	94.5(3)	O5-Dy1-Dy1A	89.54(16)
O3-Dy1A-Dy1	94.18(11)	O5-Dy1-O2A	101.74(19)
O3-Dy1A-O7A	76.7(2)	O5-Dy1-O2	81.8(2)
O3-Dy1A-N3A	100.9(2)	O5-Dy1-O3A	76.1(2)

O5A-Dy1A-Dy1	87.24(15)	O5-Dy1-N1	83.4(2)
O5A-Dy1A-O2A	79.26(19)	O5-Dy1-O7	156.1(2)
O5A-Dy1A-O2	100.7(2)	O5-Dy1-O6	150.1(3)
O5A-Dy1A-O3	78.8(2)	O5-Dy1-N3	175.7(3)
O5A-Dy1A-O6A	154.5(2)	O3A-Dy1-Dy1A	93.92(14)
O5A-Dy1A-N1A	86.0(2)	O3A-Dy1-N1	146.2(2)
O5A-Dy1A-O7A	153.8(2)	O3A-Dy1-N3	102.3(3)
O5A-Dy1A-N3A	179.4(3)	N1-Dy1-Dy1A	112.73(14)
O6A-Dy1A-Dy1	83.74(18)	N1-Dy1-N3	96.2(3)
O6A-Dy1A-O3	125.5(2)	O7-Dy1-Dy1A	87.45(16)
O6A-Dy1A-N1A	75.8(2)	O7-Dy1-O3A	127.7(2)
O6A-Dy1A-O7A	51.6(2)	O7-Dy1-N1	76.0(2)
O6A-Dy1A-N3A	25.9(3)	O7-Dy1-O6	53.2(3)
N1A-Dy1A-Dy1	112.75(15)	O7-Dy1-N3	25.9(3)
N1A-Dy1A-O3	148.36(18)	O6-Dy1-Dy1A	102.3(2)
N1A-Dy1A-O7A	110.8(2)	O6-Dy1-O3A	75.7(3)
N1A-Dy1A-N3A	94.1(2)	O6-Dy1-N1	115.8(2)
O7A-Dy1A-Dy1	103.34(16)	O6-Dy1-N3	27.3(3)
O7A-Dy1A-N3A	25.7(2)	N3-Dy1-Dy1A	94.5(2)
N3A-Dy1A-Dy1	93.24(19)	Dy1-O2A-Dy1A	109.97(17)
Dy1-O2-Dy1A	108.62(18)		

6. SHAPE program details for 1-3

Table S3. Agreement factor between the coordination polyhedron of the Dy^{III} ions in **1-3** and the various ideal polyhedral calculated by the SHAPE program.

Agreement factor for Dy^{III} ion in complexes	*TDD*-8(D_{2d})	*SAPR*-8(D_{4d})	*JSD*-8(D_{2d})
Dy^{III} in **1**	**2.590**	4.653	3.833
	2.590	4.653	3.833
Dy^{III} in **2**	**2.657**	4.470	3.906
	2.657	4.470	3.906
Dy^{III} in **3**	**1.743**	2.203	3.540
	2.304	**2.146**	4.331

TDD-8(D_{2d}) = Triangular dodecahedron

SAPR-8(D_{4d}) = Square antiprism

JSD-8(D_{2d}) = Snub diphenoid J84

7. The TGA curves of complexes 1-3

(a)

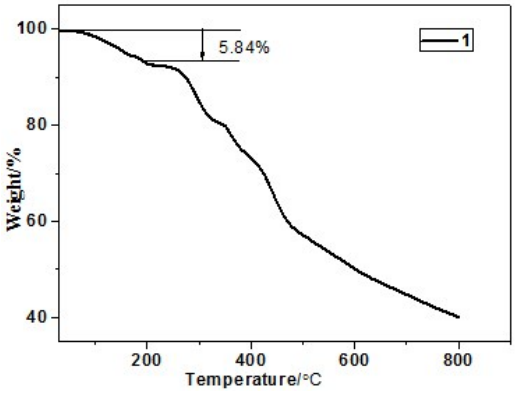

(b)

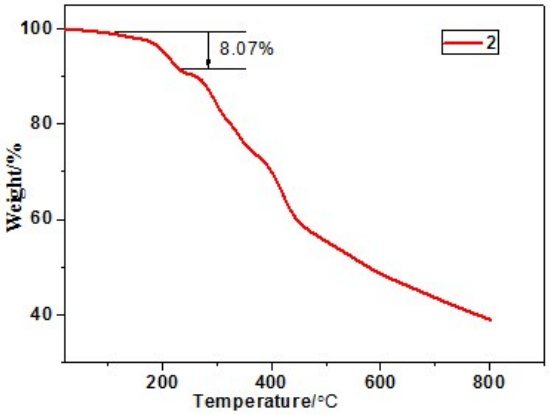

(c)

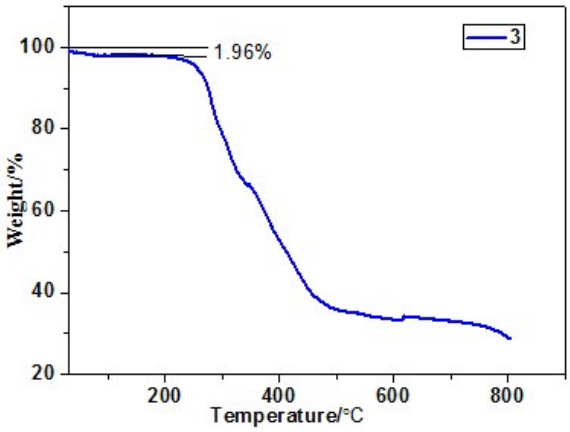

Fig. S4. The TGA curves of complexes **1** (a), **2** (b) and **3** (c).

8. Supramolecular framework of 1, 2 and 3 generated by intermolecular hydrogen-bonding interactions

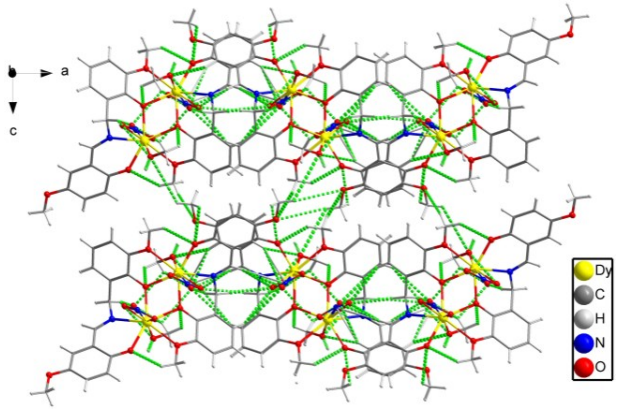

Fig. S5. 3D supramolecular framework of **1** generated by intermolecular hydrogen-bonding interactions.

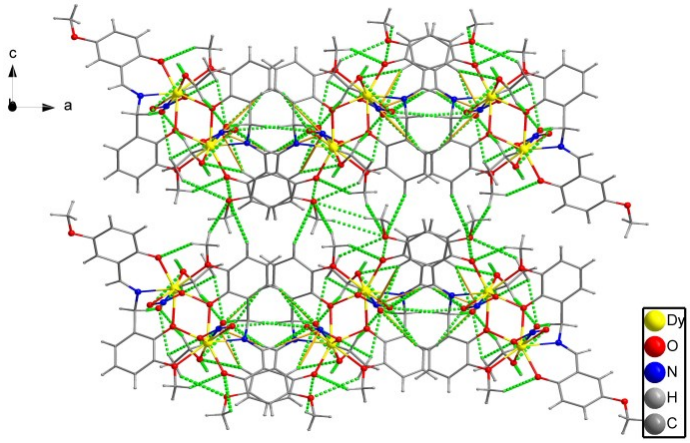

Fig. S6. 3D supramolecular framework of **2** generated by intermolecular hydrogen-bonding interactions.

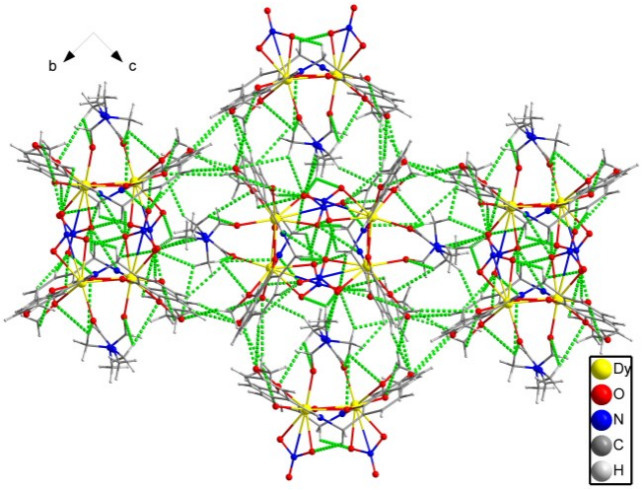

Fig. S7. 3D supramolecular framework of **3** generated by intermolecular hydrogen-bonding interactions.

9. Hydrogen-bonding parameters (Å, deg) of 1, 2 and 3

Table S4. Hydrogen-bonding parameters (Å , deg) of **1**.

D-H···A	*d*(D-H)	*d*(H···A)	D···A	∠D-H···A
C8-H8A···O8	0.970	2.544	3.439	153.56
C1-H1A···O1	0.960	2.468	3.118	124.89
O5-H5A···O4	0.853	1.948	2.769	161.28
C17-H17B···O6	0.960	2.645	3.398	135.69
C17-H17B···O8	0.960	2.320	3.221	156.14

Table S5. Hydrogen-bonding parameters (Å , deg) of **2**.

D-H···A	*d*(D-H)	*d*(H···A)	D···A	∠D-H···A
O5-H5···O4	0.857	1.977	2.825	170.41
C1-H1A···O1	0.960	2.547	3.123	118.66
C17-H17A···O8	0.970	2.307	3.233	159.49
C17-H17B···O2	0.970	2.660	3.271	121.31

Table S6. Hydrogen-bonding parameters (Å , deg) of **3**.

D-H···A	*d*(D-H)	*d*(H···A)	D···A	∠D-H···A
C9-H9A···O7	0.970	2.510	2.510	125.68
C9A-H9AA···O6A	0.970	2.524	2.524	125.33
C32-H32C···O1A	0.960	2.549	2.549	114.97
C6A-H6A···O8	0.930	2.586	2.586	129.44
C3AA-H3AC···O1	0.960	2.597	2.597	114.15
C17-H17A···O8A	0.960	2.657	2.657	142.78
C18-H18C···O8A	0.960	2.511	2.511	145.82

10. The *M* vs *H* plots for 1 (a), 2 (b) and 3 (c) at 2 k

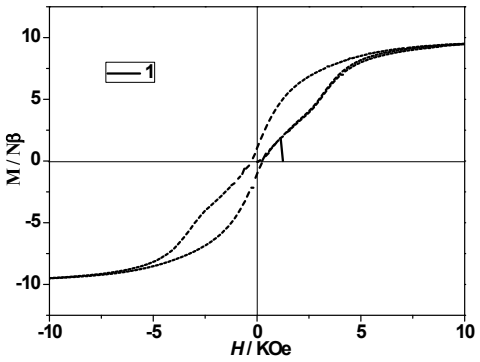

(a)

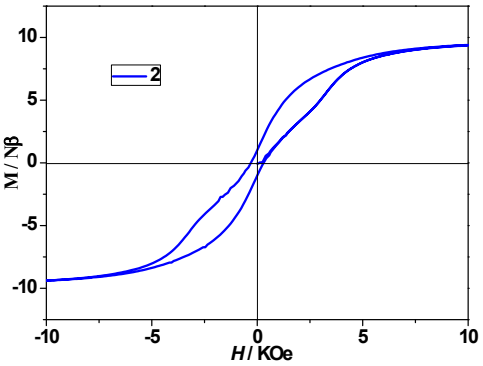

(b)

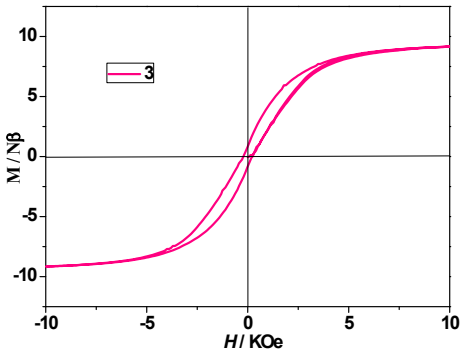

(c)

Fig. S8. Plots of magnetizations (*M*) vs dc field (*H*) for **1** (a), **2** (b) and **3** (c) at 2 K.

11. Ac susceptibilities measurements for 3 at 2-35 K in 0 Oe, 500 Oe, 1000 Oe and 2000 Oe field

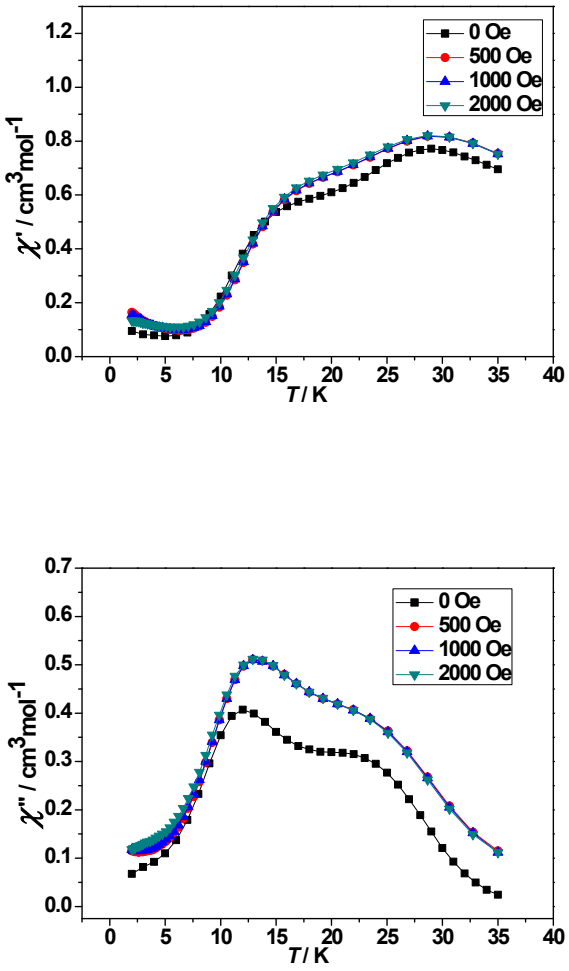

Fig. S9. Temperature dependence of the in-phase (χ′) and out-of-phase (χ″) ac susceptibility of **3** under 0 Oe, 500 Oe, 1000 Oe and 2000 Oe field in the frequency 1000 Hz at 2–35 K .

12. lnτ versus T^{-1} plots for complexes 1-3 at high temperatures

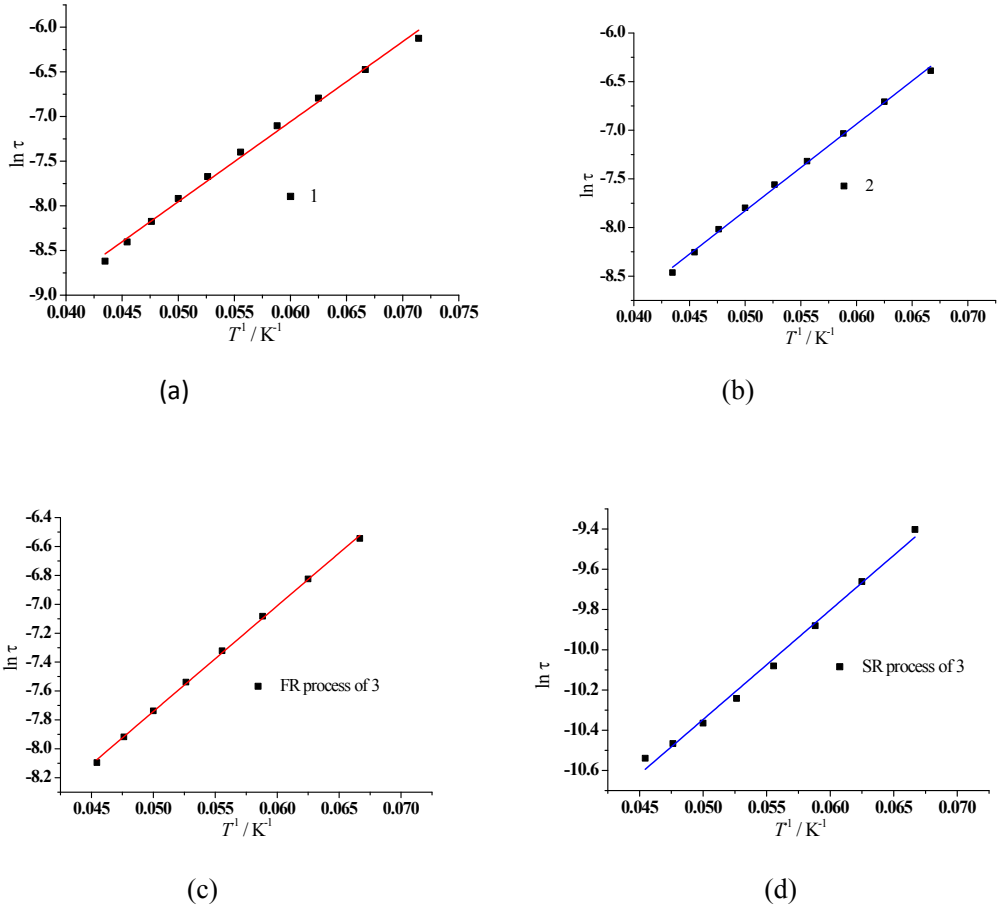

Fig. S10. lnτ versus T^{-1} plots for **1** (a), **2** (b) and **3** (c and d) at the high temperatures; the solid lines represent the least-squares fits of the experimental data to the Arrhenius law.

13. Best fitted parameters for complexes 1-3 under 0 Oe dc field

Table S7. Parameters from the fitting of the Cole-Cole plots of **1** according to the generalized Debye model.

Temperature / K	χ_s / cm^3 mol^{-1}	χ_T / cm^3 mol^{-1}	τ / s	α	*R*
12	5.11E-08	2.74E+00	5.20E-03	5.16E-02	1.06E-01
13	9.19E-08	2.45E+00	3.34E-03	4.51E-02	1.49E-01
14	1.21E-07	2.23E+00	2.19E-03	3.24E-02	3.71E-02
15	2.78E-07	2.08E+00	1.54E-03	3.41E-02	5.64E-02
16	3.25E-07	1.94E+00	1.12E-03	4.00E-02	1.36E-01
17	5.83E-07	1.81E+00	8.22E-04	3.91E-02	1.08E-01
18	1.53E-06	1.69E+00	6.12E-04	2.90E-02	1.72E-01
19	1.96E-06	1.59E+00	4.66E-04	2.60E-02	7.89E-02
20	2.55E-06	1.52E+00	3.64E-04	3.43E-02	1.86E-01
21	4.55E-07	1.42E+00	2.82E-04	1.49E-02	8.38E-02
22	6.50E-07	1.35E+00	2.24E-04	1.52E-02	1.15E-01
23	1.90E-07	1.32E+00	1.81E-04	3.33E-02	2.06E-01

Table S8. Parameters from the fitting of the Cole-Cole plots of **2** according to the generalized Debye model.

Temperature / K	χ_s / cm^3 mol^{-1}	χ_T / cm^3 mol^{-1}	τ / s	α	*R*
12	1.01E-16	3.04E+00	5.54E-03	9.96E-02	9.85E-02
13	2.44E-16	2.82E+00	3.78E-03	1.12E-01	9.22E-02
14	3.92E-16	2.54E+00	2.48E-03	1.04E-01	8.18E-02
15	6.20E-16	2.30E+00	1.68E-03	8.74E-02	1.03E-01
16	6.30E-16	2.15E+00	1.22E-03	8.57E-02	7.10E-02
17	1.01E-15	1.97E+00	8.82E-04	7.04E-02	1.94E-01
18	1.44E-15	1.84E+00	6.64E-04	6.21E-02	1.75E-01
19	2.36E-15	1.76E+00	5.21E-04	7.17E-02	1.05E-01
20	3.87E-15	1.67E+00	4.11E-04	7.13E-02	6.33E-02
21	6.54E-15	1.60E+00	3.30E-04	7.45E-02	1.06E-01
22	1.10E-14	1.50E+00	2.60E-04	5.13E-02	5.59E-02
23	1.50E-14	1.42E+00	2.11E-04	4.28E-02	5.71E-02

Table S9. Parameters from the fitting of the Cole-Cole plots of **3** according to the generalized Debye model.

8	$\chi_{s,tot}$/ cm^3 mol^{-1}	$\Delta\chi_1$/ cm^3 mol^{-1}	τ_1 / s	α_1	$\Delta\chi_2$/ cm^3mol^{-1}	τ_2 / s	α_2	R
9	1.16E-12	2.12974	0.01961	0.10728	1.36582	0.00104	0.17028	0.00475
10	1.20E-17	2.90727	0.01395	0.31370	0.73096	0.00047	0.04929	0.00341
11	4.79E-31	1.95212	0.00783	0.16634	0.93041	0.00035	0.10261	0.00132
12	7.40E-31	1.61065	0.00524	0.11920	0.93098	0.00025	0.12176	0.00105
13	5.42E-31	1.40288	0.00365	0.09594	0.89366	0.00019	0.12995	0.00092
14	9.34E-31	1.24500	0.00263	0.08133	0.85366	0.00014	0.13975	0.00114
15	2.02E-30	1.13094	0.00191	0.07415	0.80308	0.00011	0.14444	0.00147
16	1.09E-30	1.02361	0.00144	0.06543	0.76906	0.00008	0.15200	0.00119
17	2.63E-30	0.95131	0.00109	0.06184	0.71909	0.00006	0.14157	0.00109
18	4.85E-30	0.88157	0.00084	0.05563	0.68096	0.00005	0.13004	0.00094
19	1.15E-29	0.82565	0.00066	0.05064	0.64348	0.00004	0.10724	0.00083
20	1.70E-29	0.76538	0.00053	0.04372	0.62142	0.00004	0.09809	0.00069
21	2.54E-29	0.70928	0.00044	0.03646	0.60384	0.00003	0.07767	0.00056
22	4.13E-29	0.64467	0.00036	0.02722	0.60236	0.00003	0.08662	0.00049

14. Examples of Dy_2 SMMs bearing $[Dy_2O_2]$ units

Table S10. Examples of seven/eight-coordinated Dy_2 SMMs bearing $[Dy_2O_2]$ units

Complex	Solvent ligand	Donors	Dy···Dy distance/Å	Dy-O-Dy Angle/°	Magnetic behavior	Energy barrier	τ_0 (s)
$[Dy_2(L^1)_2(DBM)_2(DMF)_2]$[S1a]	DMF	NO_7	3.7900(3)	106.87(9)	F	63	2.8×10^{-11}
$[Dy_2(L^1)_2(DBM)_2(DMA)_2]\cdot2DMA\cdot2CH_3CN$[S1a]	DMA	NO_7	3.7549(4)	105.52(12)	AF	/	/
$[Dy_2(L^2)_2(DBM)_2(DMA)_2]\cdot2DMA$[S1b]	DMA	NO_7	3.7198(6)	105.3(2)	F	77	2.74×10^{-8}
$[Dy_2(L^2)_2(DBM)_2(DMF)_2]$[S1b]	DMF	NO_7	3.7270(19)	106.5(2)	F	24	1.36×10^{-6}
$[Dy_2(hmi)_2(NO_3)_2(MeOH)_2]$[S1c]	MeOH	NO_7	3.750	106.41	F	56	3×10^{-7}
$[Dy_2(L^3)_2(EtOH)_2(NO_3)_2]\cdot0.5py$[S1d]	EtOH	NO_7	3.8024(11)	109.5(2)	F	66.7	2.21×10^{-6}
$[Dy_2(L^4)_2(DBM)_2(DMA)_2]$[S1e]	DMA	NO_7		106.16(10)	AF	124	2.52×10^{-9}
$[Dy_2(L^4)_2(DBM)_2(DMF)_2]$[S1e]	DMF	NO_7		106.55(14)	AF	91	9.63×10^{-9}
$[Dy_2L^5(NO_3)2(MeOH)_2]$ [S1f]	MeOH	NO_7	3.787(5)	109.32(12)	F	198.8	2.66×10^{-7}
$[Dy_2L^5(NO_3)_2(EtOH)_2]$ [S1f]	EtOH	NO_7	3.774(1)	108.84(9)	F	131.3	2.16×10^{-6}
$[(\mu\text{-mbpymNO})\{(tmh)_3Dy\}_2]$ [S1g]	/	NO_7	7.099	/	AF	54.7	1.7×10^{-6}
		N_2O_6				47.8	1.5×10^{-8}
$[Dy_2(L^6)_2]$ [S1h]	/	N_3O_4	3.7692(3)	110.19(7)	AF	NO SMMs behavior	/
$[Dy_2(L^6)_2]\cdot MeCN$[S1h]	MeCN	N_3O_4	3.7692(5)	109.53(6)	AF	8.6	2.0×10^{-5}
$[Dy_2(bfbpen)_2(H_2O)_2]\cdot2I^-$ [S1i]	H_2O	N_4O_4	3.845	109.45	AF	20.9 26.9	3.68×10^{-6}
$[Dy_2(bcbpen)_2(H_2O)_2]\cdot2I^-\cdot0.5H_2O$ [S1i]	H_2O	N_4O_4	3.861	110.01	AF	72.7	6.79×10^{-7}
$[Dy_4(L^7)_4(MeOH)_6]\cdot2MeOH$ [S1j]	MeOH	NO_7	3.5633(2)	98.220	AF	19.7	7.8×10^{-6}
		NO_8	3.8418(2)	100.261 107.083 107.083		173	1.2×10^{-7}
$Dy_2(L^8)_2(NO_3)_2(MeOH)]_2$[this work]	MeOH	NO_7	3.7266(6)	106.4(2)	F	104	1.98×10^{-6}
$Dy_2(L^8)_2(NO_3)_2(EtOH)]_2$[this work]	EtOH	NO_7	3.7264(7)	106.84(17)	F	98.94	3.05×10^{-6}
$Dy_2(L^8)_2(NO_3)_2(DMF)_2$[this work]	DMF	NO_7	3.7987(5)	108.62(18) 109.97(17)	F	76.28 45.54	9.54×10^{-6} 3.27×10^{-6}

H_2L^1 = 2-(2-hydroxy-3-methoxy-benzylideneamino)phenol, H_2L^2 = 2-hydroxy-N'-(2-hydroxy-3-methoxybenzylidene)benzohydrazide, HDBM = dibenzoylmethane, H_2hmi = (2-hydroxy-3-methoxyphenyl)methylene(isonicotino)hydrazine, H_2L^3 = 2-(2-hydroxy-3-methoxybenzylidene)hydrazine-1-carboxylic acid, H_2L^4 = 2-naphthalen-1-ol, H_2L^5 = 2-ethoxy-6-{[(2-hydroxy-3-methoxybenzyl) imino]methyl}phenol, tmh = 2,2,6,6-tetramethyl-3,5-heptanedionate, mbpymNO = 4-methylbipyrimidine, H_2L^6 = 2-{[bis(2-hydroxy-3-ethoxybenzyl)(aminoethyl)amino]methyl}phenol), H_2bfbpen = N,N'-bis-(2-hydroxy-5-fluoro-benzyl)-N,N'-bis-(pyridin-2-ylmethyl) ethylenediamine, H_2bcbpen = N,N'-bis- (2-hydroxy-5-chloro-benzyl)-N,N'-bis-(pyridin-2-ylmethyl) ethylenedia-mine), H_2L^7 = 2-hydroxy-3-methoxybenzoicacid [(2-hydroxy-3-methoxyphenyl)methylene]hydrazide, H_2L^8 = 2-(((2-hydroxy-3-methoxybenzyl) imino)methyl)-4-methoxyphenol, F = ferromagnetic, AF = antiferromagnetic.

15. Computational details

All of binuclear complexes **1**−**3** have two types of magnetic center Dy^{III} ions indicated as **1**(**Dy1**), **1**(**Dy2**), **2**(**Dy1**), **2**(**Dy2**), **3**(**Dy1**) and **3**(**Dy2**), respectively. Complete-active-space self-consistent field (CASSCF) calculations on individual Dy^{III} fragments for **1**−**3** (see Figure S5 for the calculated complete structures of **1**−**3**) on the basis of single-crystal X-ray determined geometry have been carried out with MOLCAS 8.4[S2] program package. Each individual Dy^{III} fragment in **1**−**3** was calculated keeping the experimentally determined structure of the corresponding compound while replacing the neighboring Dy^{III} ion by diamagnetic Lu^{III}.

The basis sets for all atoms are atomic natural orbitals from the MOLCAS ANO-RCC library: ANO-RCC-VTZP for Dy^{III}; VTZ for close N and O; VDZ for distant atoms. The calculations employed the second order Douglas-Kroll-Hess Hamiltonian, where scalar relativistic contractions were taken into account in the basis set and the spin-orbit couplings were handled separately in the restricted active space state interaction (RASSI-SO) procedure. Active electrons in 7 active spaces include all *f* electrons (CAS(9 in 7) in the CASSCF calculation. To exclude all the doubts, we calculated all the roots in the active space. We have mixed the maximum number of spin-free state which was possible with our hardware (all from 21 sextets, 128 from 224 quadruplets, 130 from 490 doublets for Dy^{III}. SINGLE_ANISO[S3] program was used to obtain the energy levels, ***g*** tensors, magnetic axes, *et al.,* based on the above CASSCF/RASSI-SO calculations.

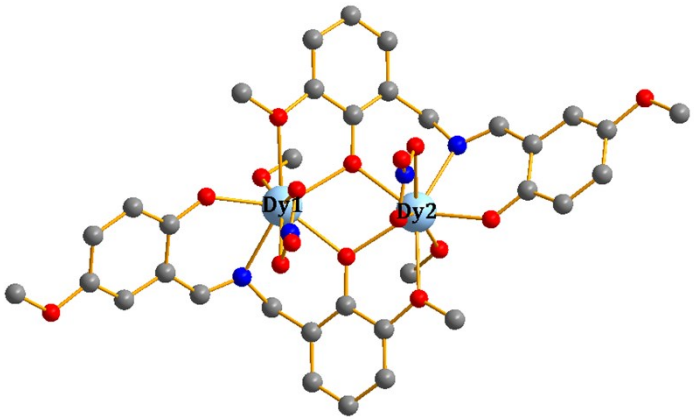

1

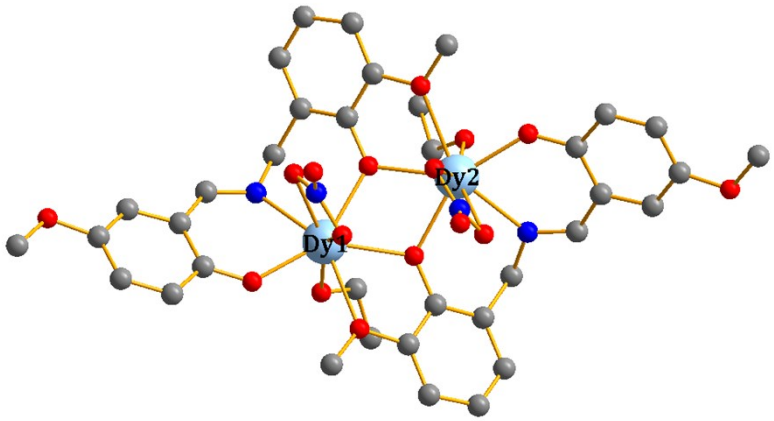

2

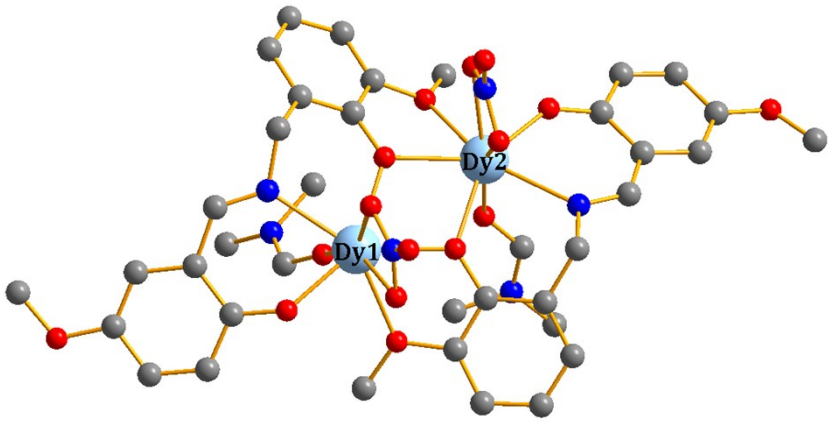

3

Fig. S11. Calculated complete structures of complexes **1**−**3**; H atoms are omitted.

Table S11. Calculated energy levels (cm^{-1}), ***g*** (g_x, g_y, g_z) tensors and predominant m_J values of the lowest eight Kramers doublets (KDs) of individual Dy^{III} fragments for complexes **1**−**3** using CASSCF/RASSI-SO with MOLCAS 8.4.

KDs	**1(Dy1)**			**1(Dy2)**			**2(Dy1)**			**2(Dy2)**		
	E/cm^{-1}	***g***	m_J	E/cm^{-1}	***g***	m_J	E/cm^{-1}	***g***	m_J	E/cm^{-1}	***g***	m_J
1	0.0	0.003 0.005 19.699	± 15/2	0.0	0.003 0.005 19.683	± 15/2	0.0	0.002 0.004 19.724	± 15/2	0.0	0.002 0.004 19.734	± 15/2
2	228.5	0.067 0.078 16.862	± 13/2	228.7	0.067 0.078 16.865	± 13/2	239.9	0.063 0.068 16.902	± 13/2	240.1	0.062 0.069 16.899	± 13/2
3	379.4	0.833 0.998 13.626	± 11/2	379.8	0.831 0.996 13.631	± 11/2	391.9	0.669 0.766 13.703	± 11/2	392.7	0.669 0.767 13.700	± 11/2

4	473.4	4.852 6.311 8.375	± 9/2	473.6	4.864 6.368 8.362	± 9/2	488.7	4.793 5.766 8.837	± 9/2	489.9	4.805 5.762 8.825	± 9/2
5	526.7	1.429 3.177 13.007	± 1/2	526.9	1.391 3.129 13.034	± 1/2	543.1	1.728 3.684 12.702	± 3/2	544.0	1.736 3.718 12.751	± 3/2
6	590.4	0.454 1.273 14.575	± 3/2	590.5	0.471 1.292 14.556	± 3/2	596.6	0.110 1.319 14.499	± 7/2	597.6	0.109 1.288 14.599	± 7/2
7	625.0	0.661 0.996 14.691	± 5/2	624.9	0.675 1.037 14.675	± 5/2	639.9	0.008 0.735 14.352	± 5/2	641.0	0.021 0.725 14.431	± 5/2
8	663.4	0.242 0.581 17.084	± 7/2	663.3	0.245 0.588 17.109	± 7/2	669.1	0.355 1.043 16.177	± 1/2	670.3	0.344 1.008 16.259	± 1/2

KDs	**3(Dy1)**			**3(Dy2)**		
	E/cm^{-1}	$\boldsymbol{g}$	m_J	E/cm^{-1}	$\boldsymbol{g}$	m_J
1	0.0	0.001 0.002 19.741	± 15/2	0.0	0.004 0.006 19.658	± 15/2
2	211.8	0.057 0.061 16.850	± 13/2	202.3	0.049 0.073 16.619	± 13/2
3	354.0	1.258 1.944 13.621	± 11/2	341.2	0.371 0.514 13.436	± 11/2
4	419.3	2.949 5.353 12.286	± 5/2	417.5	4.436 5.291 11.768	± 7/2
5	486.5	0.599 4.980 9.938	± 7/2	463.3	1.231 3.286 11.449	± 5/2
6	563.4	0.378 3.284 13.505	± 3/2	522.0	1.992 3.407 13.764	± 3/2
7	608.6	1.048 2.497 15.847	± 1/2	585.1	0.648 1.241 15.768	± 1/2
8	670.5	0.065 0.207 18.840	± 9/2	652.4	0.052 0.150 18.683	± 9/2

Table S12. Wave functions with definite projection of the total moment | m_J > for the lowest two KDs of individual Dy^{III} fragments for complexes **1**−**3**.

	E/cm^{-1}	wave functions
1(Dy1)	0.0	97.1%|±15/2>
	228.5	80.6%|±13/2>+10.7%|±9/2>+5.7%|±11/2>
1(Dy2)	0.0	97.1%|±15/2>
	228.7	80.7%|±13/2>+10.7%|±9/2>+5.7%|±11/2>
2(Dy1)	0.0	97.7%|±15/2>
	239.9	82%|±13/2>+9.7%|±9/2>+5.6%|±11/2>
2(Dy2)	0.0	97.6%|±15/2>
		81.7%|±13/2>+9.7%|±9/2>+5.8%|±11/2>
3(Dy1)	0.0	97.6%|±15/2>
	211.8	92.3%|±13/2>+3.9%|±9/2>
3(Dy2)	0.0	96.3%|±15/2>
	202.3	88.9%|±13/2>+8.8%|±9/2>

To fit the exchange interactions in complexes **1**−**3**, we took two steps to obtain them. Firstly, we calculated individual Dy^{III} fragments using CASSCF/RASSI-SO to obtain the corresponding magnetic properties. Then, the exchange interactions between the magnetic centers were considered within the Lines model,[S4] while the account of the dipole-dipole magnetic couplings were treated exactly. The Lines model is effective and has been successfully used widely in the research field of *d* and *f*-elements single-molecule magnets.[S5]

For complexes **1**−**3**, there is only one type of *J*.

The Ising exchange Hamiltonian is:

$$H_{exch} = -JS_{Dy1}S_{Dy2} \quad (1)$$

The J_{total} is the parameter of the total magnetic interaction ($J_{total} = J_{dip} + J_{exch}$) between magnetic center ions. The S_{Dy} = 1/2 is the ground pseudospin on the Dy^{III} site. The dipolar magnetic coupling can be calculated exactly, while the exchange coupling constant was fitted through comparison of the computed and measured magnetic susceptibilities using the POLY_ANISO program.[S3]

Table S13. Exchange energies E (cm^{-1}), the energy difference between each exchange doublets Δ_t (cm^{-1}) and the main values of the g_z for the lowest two exchange doublets of **1**−**3**.

	1			**2**			**3**		
	E	Δ_t	g_z	E	Δ_t	g_z	E	Δ_t	g_z
1	0.00	0.27×10^{-6}	38.252	0.00	0.97×10^{-7}	38.408	0.00	0.83×10^{-7}	39.297
2	0.61	0.42×10^{-6}	9.367	1.03	0.24×10^{-6}	9.043	0.34	0.20×10^{-6}	2.842

References:

S1 (*a*) K. Zhang, D. Liu, V. Vieru, L. Hou, B. Cui, F. S. Guo, L. F. Chibotaru and Y. Y. Wang, *Dalton Trans.*, 2017, **46**, 638-642; (*b*) K. Zhang, C. Yuan, F. S. Guo, Y. Q. Zhang and Y. Y. Wang, *Dalton Trans.*, 2016, **46**, 186-192; (*c*) P. H. Lin, T. J. Burchell, R. Clerac and M. Murugesu, *Angew. Chem., Int. Ed.,* 2008, **47**, 8848-8851; (*d*) J. Zhang, F. H. Zhang, Y. M. Chen, X. F. Zhang, Y. H. Li, W. Liu and Y. P. Dong, *Dalton Trans.*, 2016, **45**, 16463-16470; (*e*) K. Zhang, F. S. Guo and Y. Y. Wang, *Dalton Trans.*, 2017, **46**, 1753-1756; (*f*) R.-Y. Qin, H.-F. Zhang, H. Sun, Y.-D. Pan, Y. Ge, Y.-H. Li and Y.-Q. Zhang, *Chem. -Asian J.*, 2017, **12**, 2834-2844; (*g*) I. F. Díaz-Ortega, J. M. Herrera, D. Aravena, E. Ruiz, T. Gupta, G. Rajaraman, H. Nojiri and E. Colacio, *Inorg. Chem.*, 2018, **57**, 6362-6375; (*h*) Y. Ge, Y.-R. Qin, Y.-F. Cui, Y.-D. Pan, Y. Huang, Y.-H. Li, W. Liu and Y.-Q. Zhang, *Chem.-Asian J.*, 2018, **13**, 3753-3761; (*i*) X. F. Ma, B. B. Chen, Y. Q. Zhang, J. H. Yang, Q. Shi, Y. L. Ma and X. Y. Liu, *Dalton Trans.*, 2019, **48**, 12622-12631. (j) Y.-N. Guo, G.-F. Xu, P. Gamez, L. Zhao, S.-Y. Lin, R. P. Deng, J. K. Tang and H.-J. Zhang, *J. Am. Chem. Soc.*, 2010, **132**, 8538-8539.

S2 F. Aquilante, J. Autschbach, R. K. Carlson, L. F. Chibotaru, M. G. Delcey, L. De Vico, I. Fdez. Galván, N. Ferré, L. M. Frutos, L. Gagliardi, M. Garavelli, A. Giussani, C. E. Hoyer, G. Li Manni, H. Lischka, D. Ma, P. Å. Malmqvist, T. Müller, A. Nenov, M. Olivucci, T. B. Pedersen, D. Peng, F. Plasser, B. Pritchard, M. Reiher, I. Rivalta, I. Schapiro, J. Segarra-Martí, M. Stenrup, D. G. Truhlar, L. Ungur, A. Valentini, S. Vancoillie, V. Veryazov, V. P. Vysotskiy, O. Weingart, F. Zapata, R. Lindh, MOLCAS 8: New Capabilities for Multiconfigurational Quantum Chemical Calculations across the Periodic Table, *J. Comput. Chem*., 2016, **37**, 506.

S3 (*a*) L. F. Chibotaru, L. Ungur and A. Soncini, *Angew. Chem. Int. Ed.*, 2008, **47**, 4126. (*b*) L. Ungur, W. Van den Heuvel and L. F. Chibotaru, *New J. Chem.*, 2009, **33**, 1224. (*c*) L. F. Chibotaru, L. Ungur, C. Aronica, H. Elmoll, G. Pilet and D. Luneau, *J. Am. Chem. Soc.*, 2008, **130**, 12445.

S4 Lines, M. E. *J. Chem. Phys*., **1971**, *55*, 2977.

S5 (*a*) K. C. Mondal, A. Sundt, Y. H. Lan, G. E. Kostakis, O. Waldmann, L. Ungur, L. F. Chibotaru, C. E. Anson and A. K. Powell, *Angew. Chem., Int. Ed*., 2012, **51**, 7550. (*b*) S. K. Langley, D. P. Wielechowski, V. Vieru, N. F. Chilton, B. Moubaraki, B. F. Abrahams, L. F. Chibotaru and K. S. Murray, *Angew. Chem., Int. Ed*., 2013, **52**, 12014.